Blockade of a laminin-411 - Notch axis with CRISPR/Cas9 or a nanobioconjugate inhibits glioblastoma growth through tumor-microenvironment crosstalk

Tao Sun[1], **Rameshwar Patil**[1,2], **Anna Galstyan**[1], **Dmytro Klymyshyn**[1], **Hui Ding**[1,2], **Alexandra Chesnokova**[1,3], **Webster K. Cavenee**[4], **Frank B. Furnari**[4], **Vladimir A. Ljubimov**[5,6], **Ekaterina S. Shatalova**[1], **Shawn Wagner**[7], **Debiao Li**[7], **Adam N. Mamelak**[2,5], **Serguei I. Bannykh**[2,8], **Chirag G. Patil**[5], **Jeremy D. Rudnick**[2,5], **Jethro Hu**[2,5], **Zachary B. Grodzinski**[1], **Arthur Rekechenetskiy**[9], **Vida Falahatian**[10], **Alexander V. Lyubimov**[11], **Yongmei L. Chen**[11], **Lai S. Leoh**[12,13], **Tracy R. Daniels-Wells**[13], **Manuel L. Penichet**[13,14], **Eggehard Holler**[1,2,15,17], **Alexander V. Ljubimov**[2,5,16,17], **Keith L. Black**[1,2,17], and **Julia Y. Ljubimova**[1,2,5,17]

[1]Nanomedicine Research Center, Department of Neurosurgery, Cedars-Sinai Medical Center, 8700 Beverly Blvd., AHSP, Los Angeles, CA 90048, USA

[2]Samuel Oschin Comprehensive Cancer Center, Cedars-Sinai Medical Center, Los Angeles, California, USA

[3]Present address: Department of Anesthesiology and Pain Medicine, University of California Davis Health System, 2315 Stockton Blvd., Sacramento, CA 95817, USA

[4]Ludwig Institute for Cancer Research, University of California San Diego, 9500 Gilman Drive, MC-0660, La Jolla, CA 92093, USA

[5]Department of Neurosurgery, Cedars-Sinai Medical Center, 8700 Beverly Blvd., AHSP, Los Angeles, CA 90048, USA

[6]Present address: Department of Neurosurgery and Brain Repair, University of South Florida, 2 Tampa General Circle, Tampa, FL 33606, USA

[7]Biomedical Imaging Research Institute, Cedars-Sinai Medical Center, 8700 Beverly Blvd, Davis Building G149E, Los Angeles, California 90048, USA

[8]Department of Pathology and Laboratory Medicine, Cedars-Sinai Medical Center, 8700 Beverly Blvd., Los Angeles, CA 90048, USA

[9]St. George's University c/o University Support Services, LLC, The North American Correspondent 3500 Sunrise Highway, Building 300, Great River, NY 11739, USA

Corresponding author: Dr. Julia Ljubimova, Nanomedicine Research Center, Department of Neurosurgery, Cedars-Sinai Medical Center, 8700 Beverly Boulevard, AHSP-A8307, Los Angeles, CA 90048, USA. ljubimovaj@cshs.org.

[10]Duke University School of Medicine, Department of Biostatistics and Bioinformatics, Clinical Research Training Program (CRTP), 2424 Erwin Road, Suite 1102, Hock Plaza Box 2721 Durham, NC 27710, USA

[11]Toxicology Research Laboratory (TRL), Department of Pharmacology, University of Illinois at Chicago, 808 South Wood St, Chicago, IL, USA

[12]Present address: Bioprocessing Technology Institute, Immunology Group, Singapore

[13]Division of Surgical Oncology, Department of Surgery; David Geffen School of Medicine, University of California Los Angeles, 10833 Le Conte Avenue, CHS 54-140, Los Angeles, CA 90095, USA

[14]Department of Microbiology, Immunology and Molecular Genetics; David Geffen School of Medicine at University of California, Los Angeles; Jonsson Comprehensive Cancer Center, the Molecular Biology Institute, AIDS Institute, the California NanoSystems Institute, University of California Los Angeles, 10833 Le Conte Avenue, CHS 54-140, Los Angeles, CA 90095, USA

[15]Institut für Biophysik und Physikalische Biochemie, Universität Regensburg, D-93040 Regensburg, Germany

[16]Department of Biomedical Sciences, Board of Governors Regenerative Medicine Institute, Cedars-Sinai Medical Center, 8700 Beverly Blvd., AHSP, Los Angeles, CA 90048, USA

[17]These authors contributed equally to this work.

Abstract

There is an unmet need for the treatment of glioblastoma multiforme (GBM). The extracellular matrix (ECM), including laminins, in the tumor microenvironment is important for tumor invasion and progression. In a panel of 226 patient brain glioma samples, we found a clinical correlation between the expression of tumor vascular laminin-411 ($\alpha4\beta1\gamma1$) with higher tumor grade and with expression of cancer stem cell (CSC) markers including Notch pathway members, CD133, Nestin, and c-Myc. Laminin-411 overexpression also correlated with higher recurrence rate and shorter survival of GBM patients. We also showed that depletion of laminin-411 $\alpha4$ and $\beta1$ chains with CRISPR/Cas9 in human GBM cells led to reduced growth of resultant intracranial tumors in mice, and significantly increased survival of host animals compared to mice with untreated cells. Inhibition of laminin-411 suppressed Notch pathway in normal and malignant human brain cell types. A nanobioconjugate potentially suitable for clinical use and capable of crossing blood-brain barrier was designed to block laminin-411 expression. Nanobioconjugate treatment of mice carrying intracranial GBM significantly increased animal survival and inhibited multiple CSC markers including the Notch axis. This study describes an efficient strategy for GBM treatment via targeting a critical component of the tumor microenvironment largely independent of heterogeneous genetic mutations in glioblastoma.

Introduction:

Gliomas often progress from low to high grade, and are very difficult to treat, especially the most malignant type, glioblastoma multiforme (GBM), according to the classification of the

World Health Organization (WHO) (1). GBM has a very poor prognosis that has not improved in the past 30 years (1–3). Recently, gliomas have been extensively characterized by genomic and molecular marker analysis, including our work under The Cancer Genome Atlas (TCGA) project (4,5). These studies have underscored GBM heterogeneity, which may provide new targets for therapy development.

The tumor microenvironment is important for malignant growth, invasion, and escape of the immune surveillance (6). It also serves as a niche for cancer stem cells (CSCs) that are largely responsible for tumor resistance to therapy and development of recurrence (6–8). Tumor blood vessels are an integral part of this niche in gliomas and provide structural and functional support to the perivascular CSCs (7–11). These data emphasize the importance of the vascular microenvironment in glioma development and recurrence, and suggest that new therapies can target this niche for inhibiting glioma growth and CSCs (6,8,12).

We previously found that GBMs and other tumors overexpressed the vascular basement membrane protein laminin-411 ($\alpha4\beta1\gamma1$), whereas low-grade tumors and normal brain expressed laminin-421 ($\alpha4\beta2\gamma1$). These data suggest a laminin isoform shift (from $\beta2$ to $\beta1$ chain) during glioma progression (13). Laminin-411, as a progression-related tumor microenvironment marker, may be a promising therapeutic target. Uncovering the molecular ties between laminin-411, angiogenic factors, and signaling pathways that promote tumor angiogenesis and CSC survival may significantly improve brain cancer therapy. *In vitro* evidence supports the interaction of the laminin-411 $\alpha4$ chain with the Notch signaling system through the $\beta1$ integrin-Dll4 (Notch ligand) pathway (14–16). Notch-1 is overexpressed in astrocytomas, and Notch-3 is important for glioma invasion (17–19). The Notch receptor family has also been associated with CSCs (20).

In this study, we made several novel observations. (1) We documented a correlation of laminin-411 expression levels with glioma grade and CSC markers including Notch-1, Notch-3, CD133, Nestin and c-Myc in 223 human glioma samples. (2) To examine laminin-411 as a therapeutic target, we depleted its $\alpha4$ and $\beta1$ subunits with CRISPR/Cas9 system in human established and patient-derived GBM cell lines (21,22). When injected into mouse brain, GBM cells lacking laminin-411 developed smaller tumors and animal survival was significantly increased *vs.* wild type cells. (3) We developed clinically translatable treatment using nanobioconjugate inhibiting laminin-411, where all functional moieties are non-toxic, non-immunogenic (23), and with a novel chimeric tumor cell-targeting antibody applicable for human treatment. This nanodrug was able to cross blood-brain barrier and prolong survival of animals bearing intracranial GBMs. (4) Our *in vitro* and *in vivo* data supported the molecular mechanism of laminin-411 action in glioma growth through the signaling crosstalk with Notch system and CSCs, in line with new results on human tumor samples. Nanodrug inhibition or genetic ablation of laminin-411 could thus suppress GBM growth by downregulating laminin-interacting Notch system and CSCs. This study demonstrated a promising new strategy of treatment of deadly brain tumors more efficiently through targeting a critical component of tumor microenvironment, which is largely independent of the heterogeneous genetic mutations in glioblastoma.

Materials and Methods

Study approvals:

Human brain tumor and non-tumor brain tissues were obtained from patients treated at Cedars-Sinai Medical Center (CSMC; Los Angeles, CA). 223 human samples were acquired from the Biobank at the CSMC Department of Pathology & Laboratory Medicine under protocol #3646 approved by the Cedars-Sinai Institutional Review Board. Written informed consent was obtained from all donors, and the studies were conducted in accordance with the Declaration of Helsinki. Animal studies were approved by IACUC protocol #00005289.

Human brain tumor specimens:

Tumor samples included 107 GBMs, 32 grade III and 46 low-grade (I-II) gliomas (with four controls of non-tumor brain tissue from trauma patients) and were analyzed for survival and time of recurrence. Twenty-eight GBMs, six grade III, nine grade I-II gliomas, and eight non-tumor brain tissues were evaluated by immunohistochemistry (IHC) for "malignant" laminin β1 chain with CSC markers CD133, c-Myc, Notch-1, Notch-3, and Nestin.

Immunohistochemistry:

Paraffin sections were stained on a BenchMark ULTRA platform using high pH antigen retrieval and the UltraView Universal diaminobenzidine (DAB) detection kit (Ventana Medical Systems, Tucson, AZ). Frozen sections of human tumors and mouse xenogeneic tumors were stained by double indirect immunofluorescence for CSC markers and laminin β1 chain after acetone or paraformaldehyde fixation. Antibodies are listed in Supplementary Table 1. Images were captured on Leica DM6000 B microscope (Leica Microsystems, Buffalo Grove, IL) in 10 random microscopic fields/section with 40x objective, and quantitated with Leica Metamorph (MM AF 1.6) software. Nuclear objects were segregated from the DAPI signal. For CSC markers, the fraction of fluorescently positive cells was quantitated using cell scoring module. To quantitate vessel area, images were auto thresholded, regions of interest were drawn around the objects, measured, and graphed.

Cell culture:

Human GBM lines U87MG and LN229 were obtained from and authenticated by the American Type Culture Collection (ATCC, Manassas, VA) using the short tandem repeat method. LN229 cells were 100% identical to the ATCC database. U87MG were 93% identical. Patient-derived primary GBM lines, TS543 and TS576, were maintained in tumor sphere culture as published (22). Normal human brain microvascular endothelial cells (HBMVEC) were from ATCC. Normal human astrocytes (NHA) were from Lonza (Rockland, ME). All cells were routinely tested negative for mycoplasma using a kit from Lonza. Human recombinant laminin-411 and laminin-421 used for dish coating were from BioLamina (Matawan, NJ).

CRISPR/Cas9 construct and lentivirus preparation:

Lentiviral CRSISPR/Cas9 system was constructed using LentiCRISPRv2 plasmid (Addgene No. 52961) (24). Guide RNAs (gRNAs) were designed with online tool (https://

portals.broadinstitute.org/gpp/public/analysis-tools/sgrna-design), and gRNA coding sequence was inserted into LentiCRISPRv2 vector as reported (24). gRNA sequences targeting human laminin α4 gene (hg38_refGene_NM_001105206) and β1 gene (hg38_refGene_NM_002291) were as follows:

LAMA4 gRNA: GGGCACACATTCTCCCGACA;

LAMB1 gRNA: CAGGAACCCGAGTTCAGCTA

Lentiviruses were made by transfecting 293T cells with LentiCRISPRv2 construct with pseudo-viral packaging signals VSV-G and Delta-8.9 as previously reported (25).

Generation of stable laminin-411 knockout glioblastoma lines:

Human GBM lines U87MG and LN229 and patient-derived GBM lines TS543 and TS576 (22) were used to generate stable lines with laminin-411 depletion. Cells were co-infected with two lentiviral-CRISPR vectors to knock out laminin-411 α4 and β1 subunits simultaneously. Stable lines were established after 10 days of 2 μg/ml puromycin selection.

The loss of laminin-411 in lentivirus infected cells was verified by western blot and DNA sequencing. Exons targeted by CRISPR gRNAs were PCR-amplified from genomic DNA using PfuUltra II Fusion HS DNA polymerase (Agilent, Santa Clara, CA) and gel purified for Sanger DNA sequencing. PCR primers for amplification were:

LAMA4 forward: GGAGGGAAAAAGTTATGTAACAAAGAAG;

LAMA4 reverse: GCACTTGATTAGCAGTTTGCTCCTAT;

LAMB1 forward: CCCCCGCTTGTTCGTTTTTTCGG;

LAMB1 reverse: TCACCTGCAAGTGGCTGACGATACAG.

MRI Imaging of U87MG glioblastoma in nude mice:

Animals underwent MRI scanning on a 9.4 T small animal BioSpec 94/20USR scanner (Bruker Biospin MRI GmbH, Germany). Mice were placed inside a transmission whole body coil with a four-channel surface array coil (T11071 V3, Bruker Biospin MRI) positioned over the brain.

Synthesis of nanobioconjugate blocking laminin-411 expression *in vivo*:

PMLA was purified from *Physarum polycephalum* (25). Morpholino AONs 5'-AGCTCAAAGCCATTTCTCCGCTGAC-3' to laminin α4 and 5'-CTAGCAACTGGAGAAGCCCCATGCC-3' to laminin β1 chains were from GeneTools (Philomath, OR). The drug syntheses were optimized, with full characterization and toxicity evaluation (23,26). A novel recombinant mouse/human chimeric antibody targeting human transferrin receptor 1 (TfR1) with constant human IgG1 regions and variable regions of the murine monoclonal antibody 128.1, was used; it was developed similarly to the previously characterized version with IgG3 constant regions (27).

Intracranial tumor induction in nude mice:

U87MG or LN229 GBM cells were intracranially inoculated into athymic NCr-nu/nu mice obtained from Taconic (Hudson, NY) as described (28). Mice were treated with PBS or nanobioconjugate P/PEG/LLL(40%)/AON(α4β1)(2.0%)/muTfR(0.15%)/huTfRch(0.15%) with AONs against laminin-411 chains and antibodies for BBB (anti-murine TfR, muTfR) and tumor (chimeric anti-human TfR, huTfRch) targeting. Eight intravenous treatments started 8 days post tumor inoculation using 5 mg/kg AONs on every third day. Mice were euthanized on day 37 and day 48 (for U87MG and LN229, respectively) post tumor inoculation and brains were collected. Tumor volumes were calculated as (length) x (width^2)/2 (29). Western blots with tissue lysates were performed as described (28) with GAPDH or β-actin as loading controls. Antibodies are listed in Supplementary Table 1. The blots were scanned and analyzed by a LI-COR Odyssey CLx (LI-COR Biosciences, Lincoln, NE).

Competition assay

U87MG cells were trypsinized, human soluble TfR1 was added at 10-fold excess of drugs and incubated for 45–60 min at 4ºC. Fluorescently labeled full and control drugs were added to cell suspensions and incubated at 4ºC for 45–60 min. Analysis was done using flow cytometer LSR Fortessa and FACSDiva software (BD Biosciences, San Jose, CA).

Nanobioconjugate biodistribution

For tissue accumulation studies, the nanobioconjugate was labeled on tyrosines of attached antibodies with ^{125}I using Bolton-Hunter Reagent Kit (Di[^{125}I]-BHR, specific activity 577 MBq/ml; Perkin-Elmer, Waltham, MA). Twenty nude mice were intracranially inoculated with 5×10^5 U87MG GBM cells. In three weeks, ^{125}I-nanobioconjugate (~250,000 cpm; specific activity of 32,000 cpm/µg antibody) was injected once into tail vein. Six hours after injection, ~18,000 cpm/mg was incorporated in tumor tissue. Mice were euthanized at various time points (1, 2, 6, 12 and 24 hours) after injection. After PBS perfusion, brains were frozen in OCT followed by sectioning and H&E staining to locate the tumor. After background subtraction, radioactivity was calculated per mg tissue of healthy brain or tumor.

In vitro cytokine induction assay

The nanobioconjugate, along with the drug vehicle (PMLA), positive (PHA-M) and negative (PBS) controls, was tested for toxicity (cytokine release). Nanodrug was added *in vitro* to the whole blood samples from three healthy donors at therapeutic 1X dosage (based on the expected Cmax in human at the human equivalent to the mouse efficacy dose), or 3X dosage. Diluted blood was incubated with controls or nanomaterial. Using quantitative Meso Scale Discovery assay (MSD, Rockville, Maryland), nine cytokines (TNF-α, IFN-γ, IL-12p70, IL-1β, IL-2, IL-4, IL-6, IL-8, and IL-10) in the donors' blood were simultaneously measured.

Statistics: Kaplan-Meier analysis was used for animal survival studies. Patient post-diagnostic survival or recurrence was compared between laminin β1 and β2 groups

determined by immunohistochemistry using the log-rank test (Prism6 program; GraphPad Software, San Diego, CA). Differences between groups, considering unequal group sizes, were evaluated using the Tukey-Kramer multiple comparison test. Student's *t*-test was used for two groups (treated-untreated) to evaluate differences in the IHC, western blot and morphometry assays. Data are presented ± SEM, and $P < 0.05$ is considered statistically significant.

Results

Overexpression of laminin-411 is correlated with higher glioma grade and worse outcome

The expression of laminin-411 and multiple CSC markers was analyzed by immunohistochemistry in human glioma specimens. Of 107 GBMs, 92% had high levels of laminin β1 *vs.* normal brain tissue, consistent with our previous report (13) (Supplementary Table 2). Anaplastic astrocytoma grade III overexpressed laminin β1 in 67% of cases, whereas anaplastic oligoastrocytoma grade III, in 22%, which correlates with better outcome of these tumors. Only 5%, 12% and 0% cases in grade II gliomas (astrocytoma, oligodendroglioma and oligoastrocytoma, respectively) showed laminin β1 expression, and non-tumor brain tissues (n=4) were negative for laminin β1. Median survival of GBM patients (n=67) with laminin β1 overexpression was 10.0 months, and with a predominant β2 subunit it was 20.2 months (Supplementary Fig. 1A). Median time to recurrence (n=63) in GBM patients with laminin β1 was 5.6 months, whereas with laminin β2 it was 9.3 months (Supplementary Fig. 1B).

Expression of "malignant" laminin β1 chain correlates with CSC marker in human gliomas

Laminin β1 chain was found to localize to the vascular basement membrane (BM) in human gliomas (n=41; Supplementary Fig. 2A, upper row). The positive vessel area and laminin β1 staining intensity increased with glioma grade (Supplementary Fig. 2B-C; Supplementary Table 2). Because CSCs contribute to glioma progression (20), an association between high expression of laminin-411 and CSC markers was examined. In agreement with previous data (9), tumor cells positive for CSC markers (20) Notch-1, Notch-3, CD133, Nestin and c-Myc were found close to laminin β1-positive vessels, which was correlated with higher glioma progression grade (Fig. 1).

CSC marker levels were further evaluated (Supplementary Table 3). Notch-1 and Notch-3 were upregulated in high-grade gliomas (III-IV), *vs.* low-grade tumors (I-II) and non-tumor brain revealed by IHC (Fig. 1A&B) and morphometric analysis (Supplementary Fig. 3). Similar trends were observed for CD133, Nestin and c-Myc (Fig. 1C-E; Supplementary Fig. 4), and these CSC markers often co-localized with laminin β1-positive blood vessels.

Depletion of laminin-411 reduces tumor growth in vivo, enhances survival of tumor-bearing mice and suppresses Notch signaling pathway

Extracellular matrix contributes to tumor development. As laminin-411 is overexpressed during cancer progression (13), we have tested whether its loss in GBM would impair tumor growth. We disrupted laminin-411 α4 and β1 genes in two established human GBM cell lines and two patient-derived primary GBM lines TS543 and TS576 (22) using CRISPR/

Cas9 (Fig. 2A). Controls including western analysis and genomic sequencing (Fig. 2 B&C) confirmed specific elimination of laminin α4 and β1 chains. We then inoculated U87MG and LN229 cells with laminin α4 and β1 double knockout (DKO) along with their WT counterparts intracranially into nude mice (n=8 in WT groups and n=10 in DKO groups). After four weeks, tumor sizes were measured by MRI (26). Compared to WT tumors, DKO tumors were significantly smaller (Fig. 3 A&B). Consistent with imaging results, animals carrying U87MG (moderately invasive) or LN229 (highly invasive) laminin DKO tumors had significantly longer survival than animals with WT tumors (Fig. 3 C&D).

Prior studies found an interaction between laminin-411 and Notch pathway in endothelial cells (14–16). To explore this interaction in GBMs, we analyzed intracranial tumors from WT and laminin-411 DKO U87MG cells by western blot. In DKO tumors, both α4 and β1 expression remained significantly lower than their WT counterparts (Fig. 4). Notch-1, its ligand Jagged1, and another CSC marker, c-Myc, showed significantly lower expression in the laminin-411 DKO tumors (Fig. 4), suggesting that laminin-411 depletion in GBM impaired Notch and other CSC signaling pathways.

Laminin-411 upregulates the β1 integrin–Notch pathway in human endothelial cells, and in normal and malignant astrocytes

The shift of laminin isoforms from 421 (β2-containing) to 411 (β1-containing) was correlated with higher glioma grade and poor patient outcome (Supplementary Fig. 1&2). Endothelial laminin-411 interacts with the Notch system through the integrin-Dll4 pathway (15,16,30). To determine whether this interaction was functional in normal brain cells and gliomas, we conducted *in vitro* experiments to test the influence of the extracellular matrix on Notch system in normal human astrocytes (NHA), brain microvascular endothelial cells (HBMVEC), and cultured human GBM cell lines LN229 and U87MG. NHA and HBMVEC cultured on recombinant "normal" laminin-421 expressed low levels of the signaling molecules β1 integrin, Notch-1, and its ligands Jagged1 and Dll4. However, the expression of these proteins became significantly higher when cells were cultured on the "tumor" laminin-411 ($p < 0.05$), with the only exception of Jagged1 in NHA ($p = 0.05$) (Fig. 5 A&B). These data suggest functional influence of laminin-411 on the expression levels of integrin-Notch pathway members.

The link between laminin-411 and Notch pathway was further examined in cultured GBM cell lines LN229 and U87MG treated with Morpholino AONs to laminin-411 α4 and β1 chains. By western analysis, combined AONs to laminin-411 α4 and β1 inhibited the expression of their targets compared to the scrambled AON control (Fig. 5C&D). In both cell lines, suppression of laminin-411 led to significantly reduced expression of β1 integrin, Notch-1, and especially the Notch ligands Jagged1 and Dll4 (Fig. 5 C&D). Thus, laminin-411 compared to laminin-421 can upregulate the β1 integrin-Notch pathway in normal and malignant brain cells, and its inhibition downregulates this pathway. Our data on the expression of Notch and its ligands agree with juxtacrine/autocrine Notch signaling activation described for gliomas and some other cell types (31,32).

Nanodrug blocking laminin-411 efficiently treats mice bearing intracranial glioblastoma

Increased survival of animals bearing GBM with disrupted laminin-411 led us to develop a therapeutic nanobioconjugate P/PEG/LLL/AON(α4β1)/mu/huTfRch inhibiting laminin-411 by the attached AON. The nanobioconjugate structure, synthesis, characterization and mode of action are shown (Fig. 6, Supplementary Table 4, and Supplementary Video). This compound was used to treat mice with intracranial xenograft of human GBMs. The nanobioconjugate can cross BBB by endothelial transcytosis through anti-mouse TfR antibody. Tumor cell targeting and internalization are mediated by the attached new chimeric antibody against tumor-overexpressed TfR (ch128.1/IgG1, huTfRch), potentially suitable for clinical use. The functional activity of ch128.1/IgG1, conjugated for the first time together with other components to the PMLA-based nanobiopolymer was validated by flow cytometry (Supplementary Fig. 5). Specific tumor accumulation *in vivo* of the full ^{125}I-labeled nanobioconjugate was confirmed (Supplementary Fig. 6). Some controls were previously tested and found to be inefficient: (1) nanobioconjugate with AONs to laminin chains but without anti-TfR antibody showed the same animal survival as untreated group (33), and (2) nanobioconjugate with unrelated IgG1 antibody was significantly less accumulated in the GBM than the full nanodrug (34). Biodistribution of the ^{125}I-labeled nanobioconjugate showed little accumulation in normal brain within a 24-hour period but a significantly higher signal in the brain tumor (Supplementary Fig. 7).

Multiple systemic treatments of mice bearing intracranial LN229 or U87MG tumors with the nanobioconjugate significantly prolonged survival (Fig. 7A), with dramatic reduction of tumor volume as compared to the PBS treatment group (Fig. 7B). Different survival of untreated U87MG groups in this study may be due to different batches and known genetic drift under serum culture conditions (35). Western blot analysis (Fig. 7C&D) and immunohistochemistry (Supplementary Figs. 8–9) confirmed significant decrease of both laminin chains in the nanodrug treated tumors, and downregulation of integrin β1 and Notch ligand Dll4. Additionally, the ratio of cleaved to intact PARP was significantly increased, indicating elevated apoptosis in nanodrug treated tumors (Fig. 7C&D). In nanodrug treated tumors, IHC and morphometry also revealed a dramatic reduction of laminin β1 and of CSC markers Notch-1, Dll4, integrin β1 (Fig. 7D), CD133, Nestin and c-Myc *vs.* PBS control (Supplementary Figs. 8–9). These data correlated well with *in vitro* results (Fig. 5). In line with these findings, in two lines of patient-derived primary GBM cells TS543 and TS576 (22), the expression levels of Notch-1 and Jagged1 were correlated with the levels of laminin-411 expression, and when laminin-411 was depleted by CRISPR/Cas9, both these lines exhibited substantial reduction in the expression of Notch-1 and Jagged1 (Fig. 2B and Supplementary Fig. 10).

Nanobioconjugate shows no toxicity in a human blood assay

The nanobioconjugate was tested in cytokine induction assays, using human blood from three healthy donors, along with the drug vehicle (PMLA), positive (PHA-M) and negative (PBS) controls. A therapeutic 1X concentration, and even 3X elevated concentration of the nanodrug did not significantly induce any of the nine cytokines in the donors' blood (n=3, Supplementary Table 5), except for IL-8 in the 3X elevated dose group. However, this IL-8

level was still 40-fold lower than in the positive control group. Therefore, the nanobioconjugate showed virtually no toxicity.

Discussion

Laminin-411 is a vascular wall marker overexpressed in glioblastomas (36–38). In this study, we have established a strong correlation of laminin-411 overexpression with human glioma tumor grade, and with shorter survival and time to recurrence in GBMs. We then examined whether inhibiting laminin-411 in animal models would affect survival. Using CRISPR/Cas9 technology, we blocked laminin-411 expression in two human GBM cell lines and showed that mice bearing tumors with laminin-411 knockout exhibited slower tumor growth and better survival *vs.* mice carrying WT tumors. Consistent with these findings, significantly improved survival and reduced tumor burden were observed in nude mice with intracranial human GBMs treated with a nanobioconjugate blocking the expression of laminin-411 α4 and β1 chains. Our treatments are also supposed to deplete some other laminin isoforms. However, the major change in GBMs concerns upregulation of laminin-411 (13,38,39), and we thus believe that the main effect was due to laminin-411 blocking.

Our study newly established a functional link between laminin-411 and Notch pathway in both normal and malignant brain cells *in vitro*, consistent with signaling from laminin-411 *via* its binding β1 integrin to the Dll4-Notch pathway (Fig. 5&6). Accordingly, treatment of mice bearing GBMs with nanobioconjugate inhibiting laminin-411 prolonged animal survival with suppression of Notch family members Dll4, Notch-1 and Notch-3 in the residual tumors (Fig. 7; Supplementary Fig. 8&9). Laminins also contribute to cell adhesion and migration. Laminin-411 can facilitate GBM cell invasion (39), and its expression levels in patient GBMs correlate with glioma aggressiveness (Supplementary Table 2). Our data suggest an interplay between the effects of laminin-411 on glioma migration and invasion and on Notch signaling through interactions with laminin-binding integrin(s) containing β1 chain. Supporting this hypothesis, adhesion of glioma cells to laminin-411 increased the expression of both Notch system and β1-containing integrin (Fig. 5). Conversely, depletion of laminin-411 with CRISPR/Cas9 or a nanobioconjugate suppressed GBM growth and survival with downregulation of Notch system and β1 integrin.

Along with Notch, other CSC markers (20,40–42) including Nestin, CD133, and c-Myc were dramatically reduced in GBMs upon laminin-411 inhibition. These are common markers of neural stem cells and CSCs, and some of them (Nestin, Notch-1, Notch-3 and their ligands) have increased expression in gliomas (17–20). c-Myc is often activated in various tumor types including gliomas (42), and is important for cell proliferation, cell cycle progression, angiogenesis, and tumor response to immunotherapy (43).

Brain tumor CSCs reside in a perivascular niche (9) similar to neural stem cells (44,45). Our work demonstrated that inhibition of vascular BM component laminin-411, which is produced by tumor cells like many tumor ECM components (46), disrupts the perivascular CSC niche and negatively impacts CSCs, and may enhance the efficacy of glioma therapy. Overall, blocking laminin-411–Notch crosstalk by our nanobioconjugate could become a

novel glioblastoma treatment independent of genomic changes associated with tumor progression.

Notably, our experimental approach using CRISPR/Cas9 to disrupt the expression of both laminin α4 and β1 subunits demonstrated high efficiency in both established glioblastoma cell lines as well as the primary patient-derived glioblastoma cells (Fig. 2 B&C). Future development of CRISPR/Cas9-based nanodrug to regulate the expression of complex ECM components in tumor microenvironment might provide us an even more convenient and powerful approach, owing to the ease in multiplex genome engineering of this technology (47,48).

A clinically relevant advantage of the PMLA-based nanobioconjugate is its lack of toxicity despite of moieties potentially capable of inducing acute cytokine release in the blood (cytokine storm) (49). In the *ex vivo* human blood toxicity assay, the nanobioconjugate did not induce acute cytokine release. A very similar nanodrug also showed no toxicity in mice after repeated i.v. injections using the complete blood count and chemistry and metabolic panel assays (50).

Supplementary Material

Refer to Web version on PubMed Central for supplementary material.

Acknowledgments

References

1. Louis DN, et al. The 2016 World Health Organization Classification of Tumors of the Central Nervous System: A summary. Acta Neuropathologica 131, 803–820 (2016). [PubMed: 27157931]

2. Kanu OO, et al. Glioblastoma multiforme: a review of therapeutic targets. Expert Opinion on Therapeutic Targets 13, 701–718 (2009). [PubMed: 19409033]

3. Minniti G, Muni R, Lanzetta G, Marchetti P & Enrici RM Chemotherapy for glioblastoma: current treatment and future perspectives for cytotoxic and targeted agents. Anticancer Research 29, 5171–5184 (2009). [PubMed: 20044633]

4. Brennan CW, et al. The somatic genomic landscape of glioblastoma. Cell 155, 462–477 (2013). [PubMed: 24120142]

5. Ceccarelli M, et al. Molecular profiling reveals biologically discrete subsets and pathways of progression in diffuse glioma. Cell 164, 550–563 (2016). [PubMed: 26824661]

6. Jain RK Normalizing tumor microenvironment to treat cancer: Bench to bedside to biomarkers. Journal of Clinical Oncology 31, 2205–2218 (2013). [PubMed: 23669226]

7. Dimberg A The glioblastoma vasculature as a target for cancer therapy. Biochemical Society Transactions 42, 1647–1652 (2014). [PubMed: 25399584]

8. Liebelt BD, et al. Glioma stem cells: signaling, microenvironment, and therapy. Stem Cells International 2016, 1–10 (2016).

9. Calabrese C, et al. A perivascular niche for brain tumor stem cells. Cancer Cell 11, 69–82 (2007). [PubMed: 17222791]

10. Gilbert CA & Ross AH Cancer stem cells: Cell culture, markers, and targets for new therapies. Journal of Cellular Biochemistry 108, 1031–1038 (2009). [PubMed: 19760641]

11. Lathia JD, et al. Laminin alpha 2 enables glioblastoma stem cell growth. Annals of Neurology 72, 766–778 (2012). [PubMed: 23280793]

12. Jiang X, et al. Nanoparticle engineered TRAIL-overexpressing adipose-derived stem cells target and eradicate glioblastoma via intracranial delivery. Proceedings of the National Academy of Sciences of the USA 113, 13857–13862 (2016). [PubMed: 27849590]

13. Ljubimova J, et al. Association between laminin-8 and glial tumor grade, recurrence, and patient survival. Cancer 101, 604–612 (2004). [PubMed: 15274074]

14. Estrach S, et al. Laminin-binding integrins induce Dll4 expression and Notch signaling in endothelial cells. Circulation Research 109, 172–182 (2011). [PubMed: 21474814]

15. Kitajewski J Endothelial laminins underlie the tip cell microenvironment. EMBO Reports 12, 1087–1088 (2011). [PubMed: 22015689]

16. Stenzel D, et al. Endothelial basement membrane limits tip cell formation by inducing Dll4/Notch signalling in vivo. EMBO Reports 12, 1135–1143 (2011). [PubMed: 21979816]

17. Jubb AM, et al. Expression of vascular Notch ligands Delta-like 4 and Jagged-1 in glioblastoma. Histopathology 60, 740–747 (2012). [PubMed: 22296176]

18. Pierfelice TJ, et al. Notch3 activation promotes invasive glioma formation in a tissue site-specific manner. Cancer Research 71, 1115–1125 (2011). [PubMed: 21245095]

19. Xu P, et al. Differential expression of Notch family members in astrocytomas and medulloblastomas. Pathology & Oncology Research 15, 703–710 (2009). [PubMed: 19424825]

20. Bradshaw A, et al. Cancer stem cell hierarchy in glioblastoma multiforme. Frontiers in Surgery 3, 21 (2016). [PubMed: 27148537]

21. Hsu PD, Lander ES & Zhang F Development and applications of CRISPR-Cas9 for genome engineering. Cell 157, 1262–1278 (2014). [PubMed: 24906146]

22. Inda MM, et al. Tumor heterogeneity is an active process maintained by a mutant EGFR-induced cytokine circuit in glioblastoma. Genes & Development 24, 1731–1745 (2010). [PubMed: 20713517]

23. Ljubimova JY, et al. Polymalic acid-based nano biopolymers for targeting of multiple tumor markers: an opportunity for personalized medicine? Journal of Visualized Experiments 88, e50668 (2014).

24. Sanjana NE, Shalem O & Zhang F Improved vectors and genome-wide libraries for CRISPR screening. Nature Methods 11, 783–784 (2014). [PubMed: 25075903]

25. Kfoury N, et al. Cooperative p16 and p21 action protects female astrocytes from transformation. Acta Neuropathologica Communications 6, 12 (2018). [PubMed: 29458417]

26. Patil R, et al. MRI Virtual biopsy and treatment of brain metastatic tumors with targeted nanobioconjugates: nanoclinic in the brain. ACS Nano 9, 5594–5608 (2015). [PubMed: 25906400]

27. Ng PP, et al. Molecular events contributing to cell death in malignant human hematopoietic cells elicited by an IgG3-avidin fusion protein targeting the transferrin receptor. Blood 108, 2745–2754 (2006). [PubMed: 16804109]

28. Chou ST, et al. Simultaneous blockade of interacting CK2 and EGFR pathways by tumor-targeting nanobioconjugates increases therapeutic efficacy against glioblastoma multiforme. Journal of Controlled Release 244, 14–23 (2016). [PubMed: 27825958]

29. Takahashi M, et al. Isolation of a novel human gene, APCDD1, as a direct target of the β-Catenin/T-cell factor 4 complex with probable involvement in colorectal carcinogenesis. Cancer Research 62, 5651–5656 (2002). [PubMed: 12384519]

30. Li Z-Q, et al. Delta-like ligand 4 correlates with endothelial proliferation and vessel maturation in human malignant glioma. Onkologie 35, 763–768 (2012). [PubMed: 23207622]

31. Purow BW, et al. Expression of Notch-1 and its ligands, Delta-like-1 and Jagged-1, is critical for glioma cell survival and proliferation. Cancer Research 65, 2353–2363 (2005). [PubMed: 15781650]

32. Nandagopal N, Santat LA & Elowitz MB *Cis*-activation in the Notch signaling pathway. bioRxiv doi: 10.1101/313171 (2018).

33. Fujita M, et al. Inhibition of laminin-8 in vivo using a novel poly(malic acid)-based carrier reduces glioma angiogenesis. Angiogenesis 9, 183–191 (2006). [PubMed: 17109197]

34. Ding H, et al. Inhibition of brain tumor growth by intravenous poly (β-L-malic acid) nanobioconjugate with pH-dependent drug release [corrected]. Proceedings of the National Academy of Sciences of the USA 107, 18143–18148 (2010). [PubMed: 20921419]

35. Lenting K, Verhaak R, Ter Laan M, Wesseling P & Leenders W Glioma: experimental models and reality. Acta Neuropathologica 133, 263–282 (2017). [PubMed: 28074274]

36. Ishikawa T, et al. Laminins 411 and 421 differentially promote tumor cell migration via α6β1 integrin and MCAM (CD146). Matrix Biology 38, 69–83 (2014). [PubMed: 24951930]

37. Kawataki T, et al. Laminin isoforms and their integrin receptors in glioma cell migration and invasiveness: Evidence for a role of α5-laminin(s) and α3β1 integrin. Experimental Cell Research 313, 3819–3831 (2007). [PubMed: 17888902]

38. Nagato S, et al. Downregulation of laminin α4 chain expression inhibits glioma invasion *in vitro* and *in vivo*. International Journal of Cancer 117, 41–50 (2005). [PubMed: 15915502]

39. Khazenzon NM, et al. Antisense inhibition of laminin-8 expression reduces invasion of human gliomas in vitro. Molecular Cancer Therapeutics 2, 985–994 (2003). [PubMed: 14578463]

40. Magee JA, Piskounova E & Morrison SJ Cancer stem cells: Impact, heterogeneity, and uncertainty. Cancer Cell 21, 283–296 (2012). [PubMed: 22439924]

41. McLendon RE & Rich JN Glioblastoma stem cells: A neuropathologist's view. Journal of Oncology 2011, 1–8 (2011).

42. Wang J, et al. c-Myc is required for maintenance of glioma cancer stem cells. PLoS One 3, e3769 (2008). [PubMed: 19020659]

43. Casey SC, et al. MYC regulates the antitumor immune response through CD47 and PD-L1. Science 352, 227–231 (2016). [PubMed: 26966191]

44. McCarty JH Cell adhesion and signaling networks in brain neurovascular units. Current Opinion in Hematology 16, 209–214 (2009). [PubMed: 19318941]

45. Tavazoie M, et al. A specialized vascular niche for adult neural stem cells. Cell Stem Cell 3, 279–288 (2008). [PubMed: 18786415]

46. Socovich AM, & Naba AThe cancer matrisome: From comprehensive characterization to biomarker discovery. Seminars in Cell & Developmental Biology doi: 10.1016/j.semcdb. 2018.06.005 (2018).

47. Sakuma T, Nishikawa A, Kume S, Chayama K & Yamamoto T Multiplex genome engineering in human cells using all-in-one CRISPR/Cas9 vector system. Scientific Reports 4, 5400 (2014). [PubMed: 24954249]

48. Thakore PI, et al. RNA-guided transcriptional silencing in vivo with S. aureus CRISPR-Cas9 repressors. Nature Communications 9, 1674 (2018).

49. Wolf B, et al. A whole blood in vitro cytokine release assay with aqueous monoclonal antibody presentation for the prediction of therapeutic protein induced cytokine release syndrome in humans. Cytokine 60, 828–837 (2012). [PubMed: 22986013]

50. Ljubimova JY, et al. Toxicity and efficacy evaluation of multiple targeted polymalic acid conjugates for triple-negative breast cancer treatment. Journal of Drug Targeting, 21, 956–967 (2013). [PubMed: 24032759]

Significance statement: Laminin-411 expression in the glioma microenvironment correlates with Notch and other cancer stem cell markers and can be targeted by a novel, clinically translatable nanobioconjugate to inhibit glioma growth.
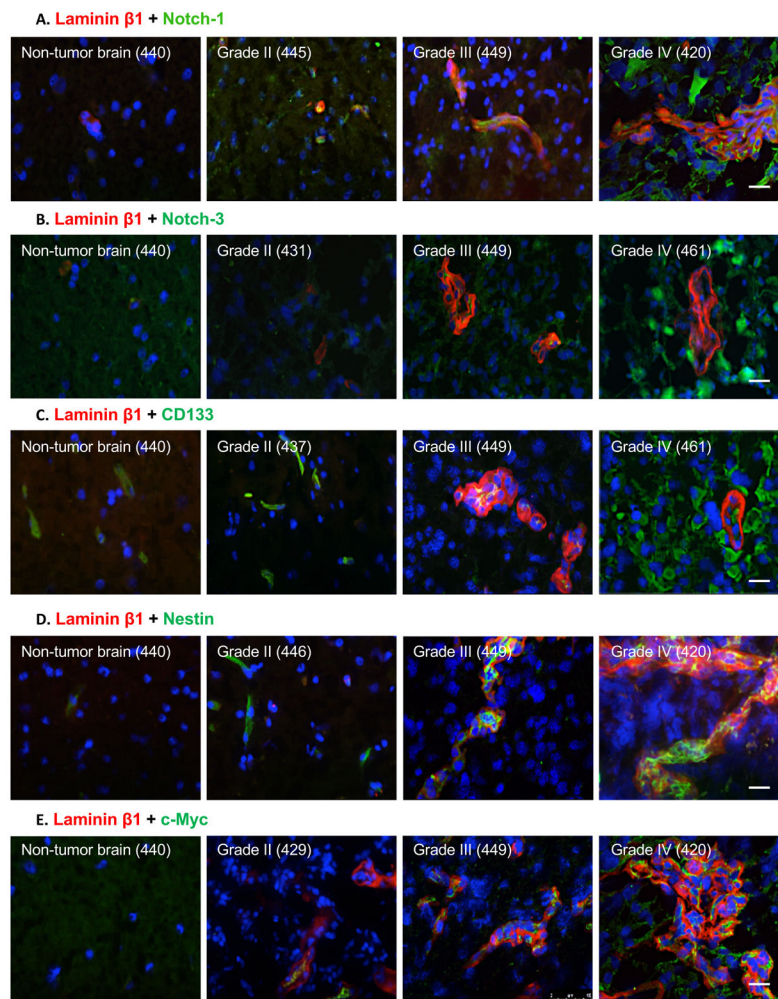
Fig. 1. Cancer stem cell markers Notch-1, Notch-3, CD133, Nestin and c-Myc are highly expressed in high-grade human gliomas.

Representative images of double labeling for laminin β1 and CSC markers: **A,** Notch-1; **B,** Notch-3; **C,** CD133; **D,** Nestin; and **E,** c-Myc in fresh-frozen human brain samples analyzed by immunofluorescence. Non-tumor human brain tissue was used as a control. The expression of Nestin and c-Myc was found both close to and far from vessels positive for laminin β1 staining. Note weak to no staining for all markers in non-tumor brain and markedly increased expression in WHO grade IV gliomas (glioblastomas). All scale bars = 25 μm. Abbreviations: CSC, cancer stem cell; WHO, World Health Organization. Numbers refer to individual patients.
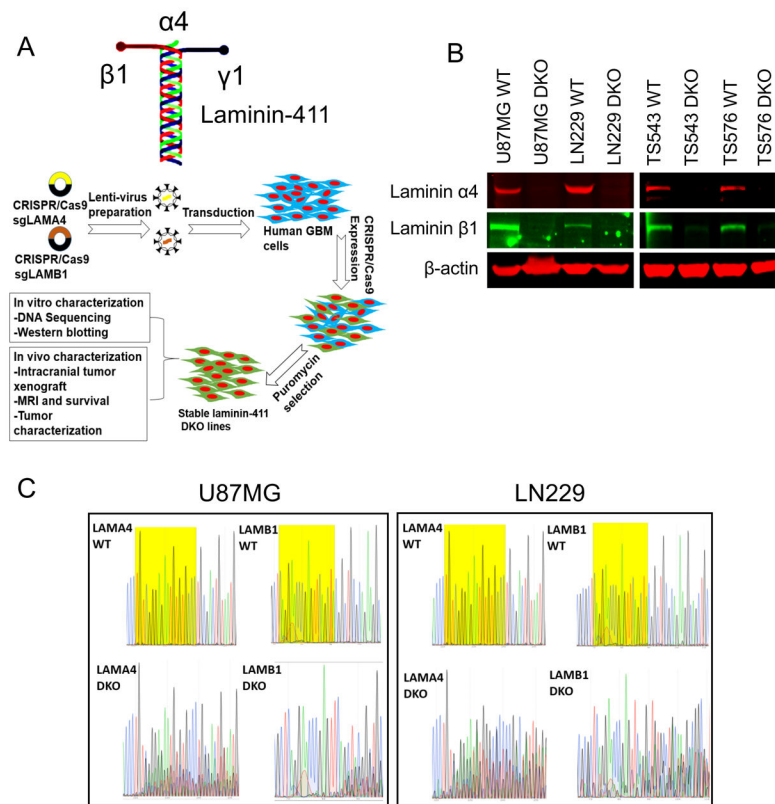
Fig. 2. Disruption of laminin-411 α4 and β1 subunits expression by CRISPR/Cas9 in established and patient-derived glioblastoma cells.
A. Schematic structure of laminin-411(α4β1γ1) complex and the workflow for α4 and β1 knockout using lentiviral CRISPR/Cas9 system; **B**. Verification of loss of laminin-411 α4 and β1 expression by western blot in GBM cell lines U87MG and LN229 as well as in two patient-derived primary glioblastoma lines TS543 and TS576; **C**. Traces of Sanger sequencing indicating disruption of laminin-411 α4 and β1 genes in both U87MG and LN229 cells. Exons of human *LAMA4* and *LAMB1* genes targeted by CRISPR gRNAs are PCR-amplified from both WT and laminin-411 DKO cells. Near the gRNA binding sites (highlighted in yellow), DKO samples showed multiple overlapping reads at almost any given loci, indicating the consequence of error-prone NHEJ DNA damage repair. None of these peaks was present in the WT samples.
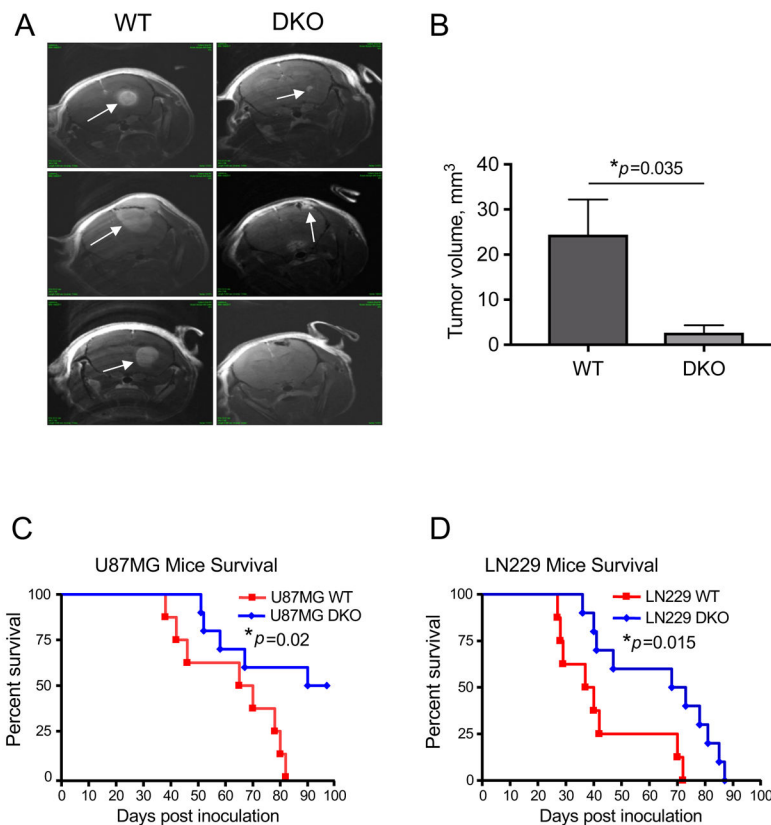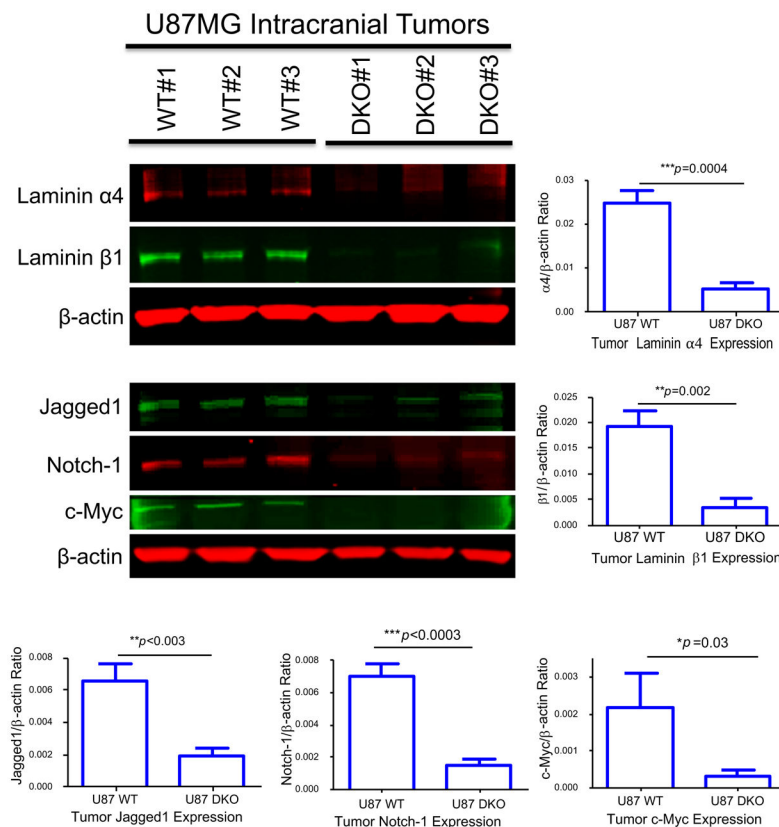
Fig. 3. Loss of laminin-411 expression in glioblastoma cells significantly decreases *in vivo* tumor burden and prolongs survival of tumor-bearing mice.

A. Magnetic resonance imaging (MRI) was performed to assess the brain tumor volume in nude mice carrying U87MG cells four weeks after intracranial tumor inoculation. Spin-echo MRI images of the entire brain were acquired from three mice/group, and representative images from mice carrying WT (n=3) *vs.* laminin-411-DKO (n=3) U87MG gliomas (marked by arrows) are shown. **B.** Quantification of intracranial tumor volumes derived from WT vs. laminin-411 DKO U87MG cells. (*p = 0.035 by two-tailed Student's *t*-test; n = 3). **C & D.** Survival curves of mice bearing human glioblastoma U87MG (C) and LN229 cells (D). Kaplan-Meier analyses showed mice with the laminin-411 α4 and β1 DKO tumors exhibited a significantly longer survival than mice carrying the WT glioblastoma cells in both U87MG (median survival WT 67 days (n=8) *vs.* DKO 93 days (n=10); *p = 0.02 by log rank test) and LN229 cohorts (median survival WT 38 days (n=8) vs. DKO 70 days (n=10); *p = 0.015 by log rank test).

Fig. 4. Characterization of intracranial tumors derived from both WT and laminin-411 DKO U87MG cells by western blot.

Intracranial tumors were dissected from mice inoculated with either WT or the laminin-411 DKO U87MG cells. Tumor samples were collected from three animals per group at the endpoint of their survival and total lysates were used for western blotting analysis. Upper blot: Levels of laminin-411 α4 and β1 in U87MG tumors (WT *vs.* laminin-411 DKO. Compared to the WT U87MG tumors, the laminin-411 α4 and β1 levels remained significantly lower in DKO tumors; Lower blot: Levels of CSC markers in the tumor samples. Notch-1, Jagged1 as well as the CSC regulator c-Myc are significantly lower than in the WT tumors.
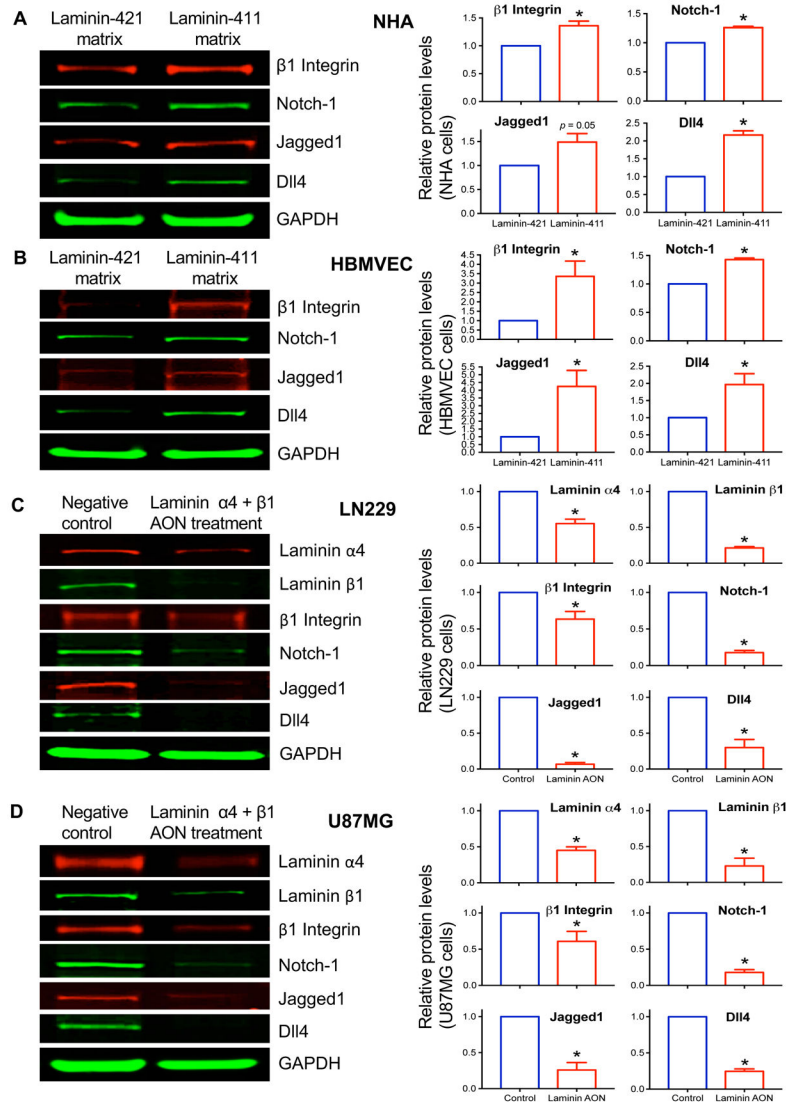
Fig. 5. Upregulation of integrin-Notch pathway by substrate-bound laminin-411 in normal brain astrocytes and endothelial cells and suppression of this pathway in cultured glioma cells by laminin-411 inhibition.

Western blots (left panels) for β1 integrin, Notch-1, Jagged1 and Dll4 expression in **A**, normal human astrocytes (NHA); and **B**, human brain microvascular endothelial cells (HBMVEC) cultured on either laminin-411 (malignant) matrix or laminin-421 (non-malignant) matrix for 3 days. Laminin-411 increased the expression of the integrin-Notch signaling pathway members in both NHA and HBMVEC, as compared with laminin-421. Blot quantitation of expression in NHA and HBMVEC using LI-COR software with the Prism 6 program shows statistically significant differences in marker expression between laminin isoforms. Only Jagged1 in NHA did not reach significance ($p = 0.05$). Antisense inhibition of laminin-411 α4 and β1 chains in cultured human glioblastoma cell lines **C**, LN229; and **D**, U87MG caused downregulation of downstream Notch signaling including β1 integrin, Notch-1, Jagged1 and Dll4. This downregulation was statistically significant. Bar graphs show fold changes (red bars) *vs.* a control group defined as 1.0. Data are

normalized to levels of glyceraldehyde 3-phosphate dehydrogenase (GAPDH) used as a loading control. * $p < 0.05$ by 2-tailed Student's t-test.
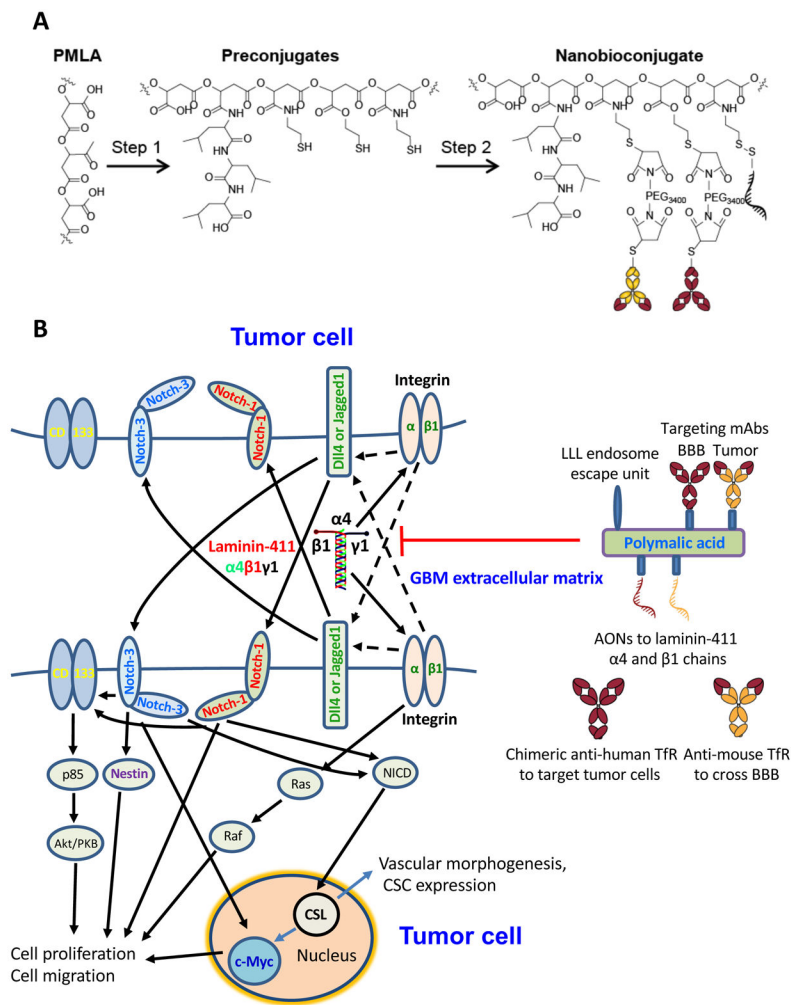
Fig. 6. Nanobioconjugates design, synthesis and schematic mechanism of drug action.
A. Nanodrug synthesis step 1: Poly(β-L-malic acid) (PMLA) was treated with a mixture of
N-hydroxysuccinimide ester (NHS) and N,N′-dicyclohexylcarbodiimide (DCC) followed by
sequential addition of trileucine (leucyl-N-leucyl-N-leucine [LLL]) peptide along with
triethanolamine (TEA) and finally 2-mercapto-1-ethylamine (MEA) followed by TEA to
form Preconjugate-1. Step 2: Monoclonal antibodies (mAbs) were functionalized with
MAL-PEG-MAL and attached to the preconjugate by a thioether. Similarly, antisense
oligonucleotides (AONs) were modified with a thiol reacting linker and attached to the
preconjugate through a disulfide linkage. The cartoon schematic of the full
nanobioconjugate is depicted at the lower left. Abbreviations: MAL, maleimide; PEG,
polyethylene glycol; PEG_{3400}, PEG with m.w.=3,400; BBB, blood-brain barrier; a-TfR,
anti-transferrin receptor mAb. **B.** Schematic of Notch signaling and nanodrug action. Left,
laminin-411 in the glioblastoma ECM interacts with β1 integrin on the tumor cell surface to
upregulate Notch ligands, e.g., delta-like 4 (Dll4). This in turn activates Notch receptors by a
juxtacrine or autocrine regulation documented in gliomas (31,32) (juxtacrine *trans*-signaling
is shown). After Notch cleavage and release of Notch intracellular domain (NICD), the
signal is transferred to the nucleus with activation of DNA-binding adaptor CSL/CBF-1,

resulting in increased transcription and CSC proliferation and expansion. Interaction with and activation of additional CSC markers CD133, Nestin and c-Myc, leads to higher proliferation, migration and vascular morphogenesis. Right, therapeutic nanobioconjugate blocking laminin-411 chain expression. It has PMLA backbone with covalently attached components: morpholino AONs inhibiting laminin α4 and β1 chain synthesis; multiple residues of trileucine (LLL) functioning as a pH-sensitive endosome escape unit for the release of AON into the tumor cell cytoplasm; BBB and tumor targeting antibodies: anti-mouse TfR mAb targeting mouse endothelial cells in tumor vessels for the nanodrug BBB crossing by transcytosis, and chimeric anti-human TfR mAb enabling drug targeting and binding to human tumor cells with subsequent receptor-mediated internalization (see Supplementary Video).
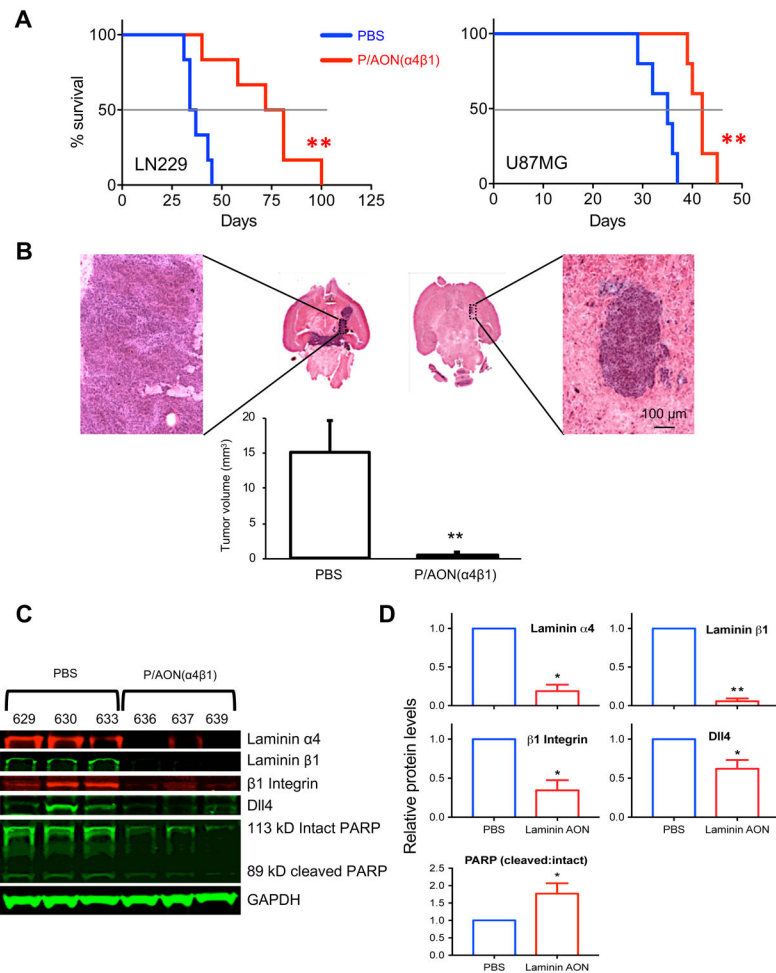
Fig. 7. Laminin-411 inhibition after nanobioconjugate treatment improves survival, reduces tumor size, and suppresses Notch signaling pathway in tumors.

A, Kaplan-Meier plots show significantly improved survival of mice bearing intracranial gliomas LN229 (left) and U87MG (right) after treatment with nanobioconjugate P/PEG/LLL/muTfR/huTfRch/AON(α4β1). For LN229, median survival time was increased significantly in nanobioconjugate treated vs. PBS group (77 *vs.* 36 days; $p < 0.004$, log-rank test). For U87MG, median survival time also increased by nanobioconjugate treatment vs. PBS control mice (42 *vs.* 35 days; $p < 0.002$). **B**, Graph shows dramatic reduction of LN229 tumor volume after nanodrug treatment as compared to PBS control group (n=6 in each group). Scale bar = 100 μm. **C**, Western blot analysis revealed diminished expression of laminin α4, laminin β1, β1 integrin and Dll4 in *ex vivo* LN229 tumor tissues from three individual nanobioconjugate-treated mice (numbers refer to individual animals) *vs.* three individual PBS mice. The ratio of cleaved poly (ADP-ribose) polymerase (PARP) to intact PARP was significantly increased after nanobioconjugate treatment indicating enhanced apoptosis in tumors. **D**, Quantification of western blots revealed significant inhibition of all components in LN229 glioma-bearing mice after nanobioconjugate treatment compared to control. Graphs show fold changes *vs.* PBS control group defined as 1.0. Data are normalized to glyceraldehyde 3-phosphate dehydrogenase (GAPDH) levels used as a

loading control in all blots. Student's *t*-test was used for comparisons, with ** $p < 0.01$; * $p < 0.05$.